Available on CMS information server

**CMS NOTE-2008/026**

**The Compact Muon Solenoid Experiment**

**CMS Note**

Mailing address: CMS CERN, CH-1211 GENEVA 23, Switzerland

**29 August 2008**

# ME1/1 Cathode Strip Chambers

Yu.V. Erchov, I.A. Golutvin, A.Yu. Kamenev, V.Yu. Karjavin, S.V. Khabarov, P.V. Moissenz, K.P. Moissenz, S.A. Movchan, V.V. Perelygin, S.E. Vassiliev, A.V. Zarubin

(Joint Institute for Nuclear Research, Dubna, Russia)

V.A. Tchekhovski

(National Scientific and Educational Center of Particle and High Energy Physics, Belarusian State University, Minsk, Belarus)

**Abstract**

The 76 innermost ME1/1 cathode strip chambers (CSC) of the CMS Experiment were designed and produced in Dubna. The chambers have been installed in the detector and commissioning has been completed. This paper describes the design of the CSCs, their main mechanical parameters and readout electronics, and the results of tests with cosmic-ray muons.

## 1. Introduction

The innermost ring of muon detectors in the CMS endcap muon system [1, 2] is called ME1/1 (Fig. 1). The ring in each endcap is composed of 36 six-layer cathode strip chambers (CSC) [3]. The chambers are positioned in the gap between the endcap hadron calorimeter (HE) and the YN1 support disk. A number of full-scale prototypes of ME1/1 CSC were designed and constructed at the Joint Institute for Nuclear Research (JINR) in Dubna [4, 5]. We carried out a comprehensive study of the prototypes by using cosmic-ray muons and the CERN SPS muon beams [6-9]. This paper describes the design of the ME1/1 CSC, which was optimised for mass-production, the main mechanical parameters of the chambers, their readout electronics, and the results of cosmic-ray muon tests.

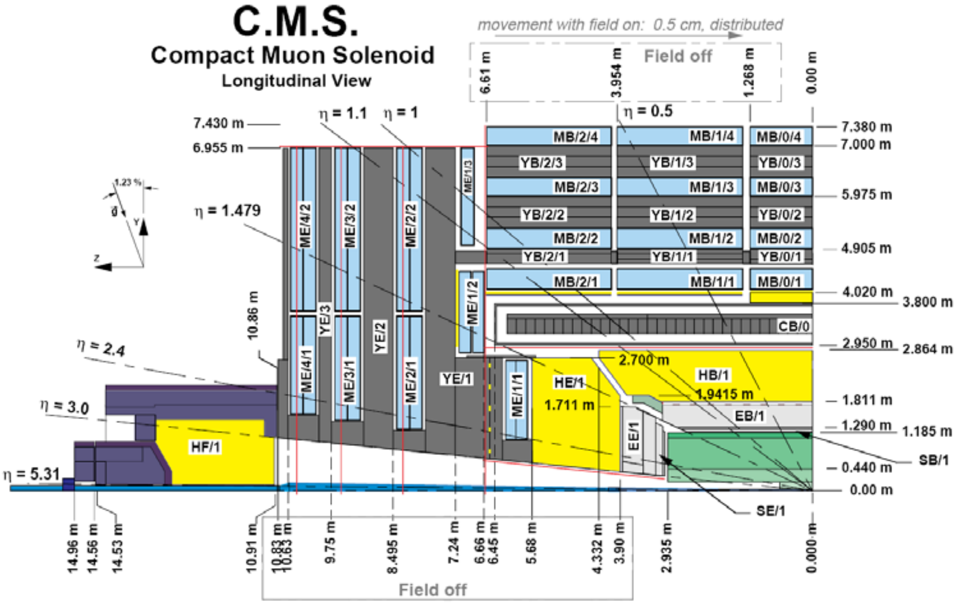


**Figure 1:** CMS cross section, quarter-view.

## 2. Layout and main parameters of the ME1/1 CSCs

One ME1/1 CSC covers 10° in φ [2, 4] and consists of 6 identical trapezoidal-shaped proportional chambers, called layers, each with cathode strip readout. Each layer is formed by 2 cathode electrodes, one divided into strips and the other a continuous plane, with a gap of 7 mm between them. A plane of anode wires is placed in the middle of the gap (Fig. 2). The chamber is composed of the 7 construction elements – panels. The basic chamber parameters are shown in Table 1.

The radial strip structure is made on Ditron 0.8 mm FR4 lists with 18 μm Cu lamination. The strips start at R=1060 mm and end at 2565 mm, covering an angle of φ = ±5.42° to provide the overlap with the neighboring CSCs in CMS endcaps (Fig. 3).

Deterioration of the CSC spatial resolution due to the presence of the magnetic field is partially compensated by wires inclination [8]. The average value of the field in ME1/1 CSCs is estimated as 3T, so the anode wires are inclined at an angle of 29° with respect to the perpendicular of the chamber axis. Groups of 11 anode wires are connected to 1 readout channel to provide the radial coordinate measurement, while the interpolation of charges induced on the strips gives a precise measurement of the φ-coordinate [10-13].

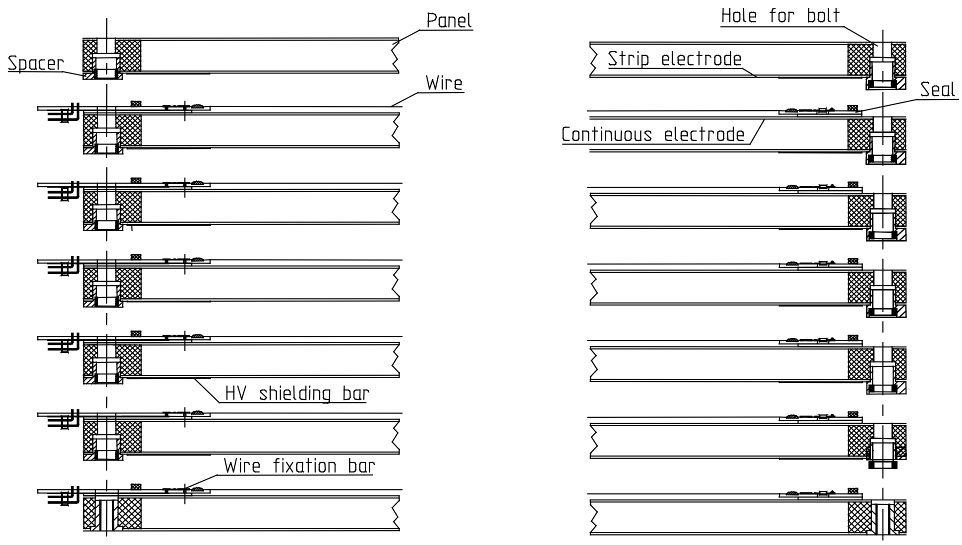


**Figure 2:** ME1/1 CSC cross-section (exploded view).

The background rate at the narrow part of the chamber is expected to be significantly higher than at the wide part [14, 15]. To decrease the counting rate per channel of the strip readout electronics, the cathode strips are mechanically separated by a cut (R=1500 mm) into 2 groups: the wide part with length of 1065 mm and the narrow part with 440 mm (Fig. 3; Table 1). Table 2 represents the sensitive area corresponding to the anode wire groups from 1 (narrow part) to 48 (wide part).

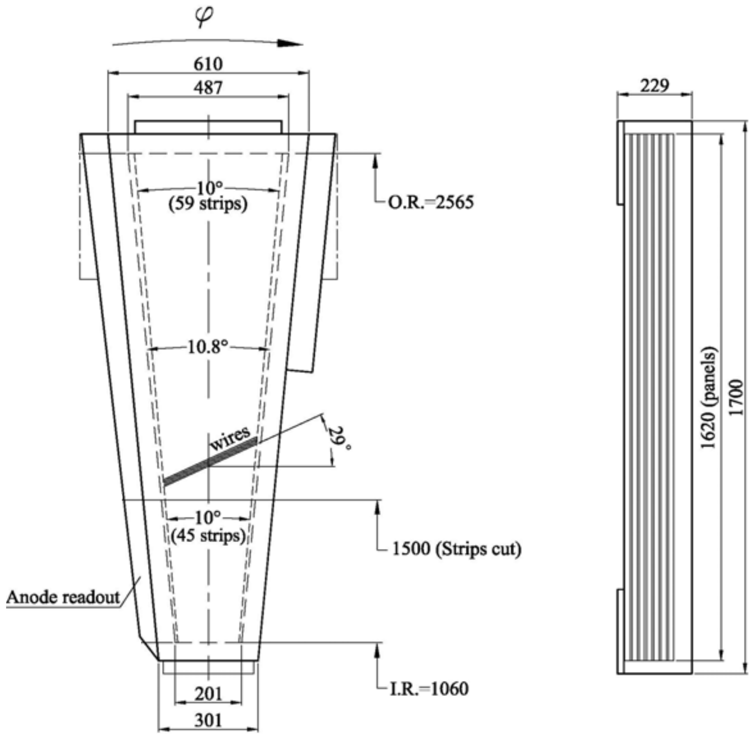


**Figure 3:** Overall dimensions of the ME1/1 CSC (in mm).

The ME1/1 CSC panel design and strip layout are similar to the P4 prototype [5]. The CSC assembly procedure is mostly the same as described in [5, 9]. The control procedure of the CSC mechanical parameters is described in [16].

**Table 1:** ME1/1 CSC parameters

| | | | |
|---|---|---|---|
| **ME1/1 CSC** | Layers / CSC | | 6 |
| | Inner radius | m | 0.965 |
| | Outer radius | m | 2.665 |
| | Strip channels | | 480 |
| | Anode channels | | 288 |
| | Gas volume | L | 25 |
| | Weight with electronics | kg | 135 |
| **CSC Layer** | Anode-Cathode gap | mm | 3.5 |
| | **Panel:** | | |
| | Height | m | 1620 |
| | Narrow part width | m | 0.301 |
| | Wide part width | m | 0.610 |
| | Thickness | mm | 15 |
| | Area | $m^2$ | 0.73 |
| | Sensitive area | $m^2$ | 0.52 |
| | **Cathode strips:** | | |
| | Shape | | Radial |
| | Number of strips: | | |
| | Wide part | | 64 |
| | Narrow part | | 48 |
| | Readout strip pitch width: wide part | mrad | 2.96 |
| | : narrow part | mrad | 3.88 |
| | Strip length: wide part | mm | 1065 |
| | : narrow part | mm | 440 |
| | **Anode wires:** | | |
| | Diameter | μm | 30 |
| | Wire Spacing | mm | 2.5 |
| | Number of wires | | 587 |
| | Number of channels | | 48 |
| | Wires / group (except gr.1 & 48) | | 11 |
| | Incline angle | degree | 29 |

**Table 2:** Anode wire group area

| Anode group number | Anode group area ($mm^2$) |
|---|---|
| 1 | 12650 |
| 2 | 6800 |
| 3 | 6988 |
| 4 | 7176 |
| 5 | 7364 |
| 6 | 7553 |
| 7 | 7741 |
| 8 | 7929 |
| 9 | 8117 |
| 10 | 8306 |
| 11 | 8494 |
| 12 | 8682 |
| 13 | 8870 |
| 14 | 9059 |
| 15 | 9247 |
| 16 | 9435 |
| 17 | 9623 |
| 18 | 9812 |
| 19 | 10000 |
| 20 | 10188 |
| 21 | 10376 |
| 22 | 10565 |
| 23 | 10753 |
| 24 | 10941 |
| 25 | 11129 |
| 26 | 11318 |
| 27 | 11506 |
| 28 | 11694 |
| 29 | 11882 |
| 30 | 12071 |
| 31 | 12259 |
| 32 | 12447 |
| 33 | 12635 |
| 34 | 12824 |
| 35 | 13012 |
| 36 | 13200 |
| 37 | 13388 |
| 38 | 13577 |
| 39 | 13765 |
| 40 | 13953 |
| 41 | 14141 |
| 42 | 14330 |
| 43 | 14412 |
| 44 | 13134 |
| 45 | 11439 |
| 46 | 9745 |
| 47 | 8051 |
| 48 | 15213 |

## 3. Readout electronics

The ME1/1 on-chamber electronics layout is shown schematically in Fig. 4. Signals from the cathode strips are amplified and shaped by five 96-channel Cathode Front End Boards (CFEB) [17, 18]. Each CFEB reads out a "tower" of 16 strips from 6 layers. There are 4 CFEBs on the wide part of a CSC and only 1 on the narrow part, thus the 48 strips in each layer of the narrow part are readout by 16 channels by the following scheme:

Ch. 1: strips 1, 17, and 33 … Ch. 16: strips 16, 32, and 48.

Therefore 3 strips connect to 1 CFEB input in the narrow part while 1 CFEB channel corresponds to 1 strip in the wide part.

Signals from the anode wires are amplified and discriminated by the Anode Front End Boards (AFEB) [19]. Each AFEB reads out 16 wire groups from 2 layers of the CSC. The discriminator bits are transmitted to the Anode Local Charge Track board (ALCT) where signals are stored as hits. An ALCT board reads out all 18 AFEBs.

The low voltage distribution board (LVDB) supplies the on-chamber electronics with stabilized low voltage.

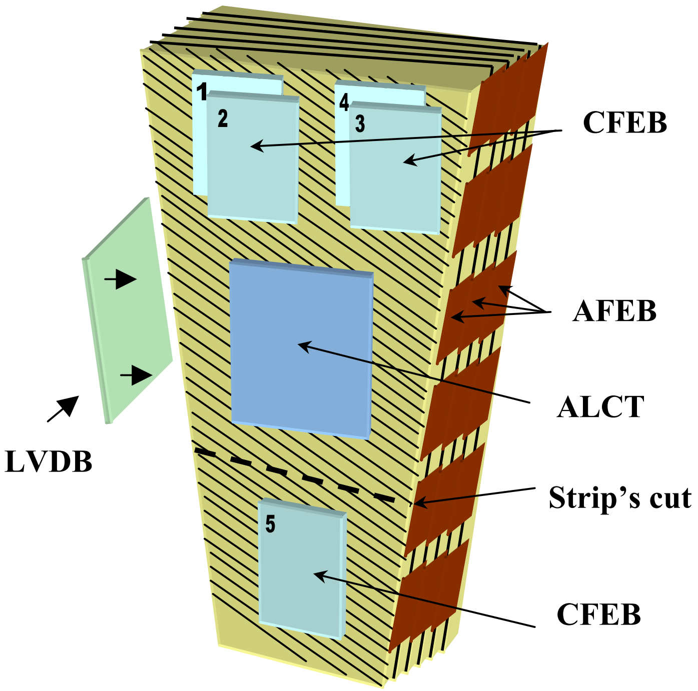


**Figure 4:** ME1/1 on-chamber electronics.

## 4. Cosmic test after CSC assembling

In Dubna, a cosmic test stand was constructed to test CSC with cosmic-ray muons (Fig. 5). It consists of upper and lower scintillation hodoscopes (1) and a 0.5 m thick iron muon filter (3). The CSC (2) to be tested is placed on a carriage on the iron filter. The test setup also includes high voltage and low voltage systems, trigger electronics, data acquisition system (DAQ), gas mixer, and water-cooling system.

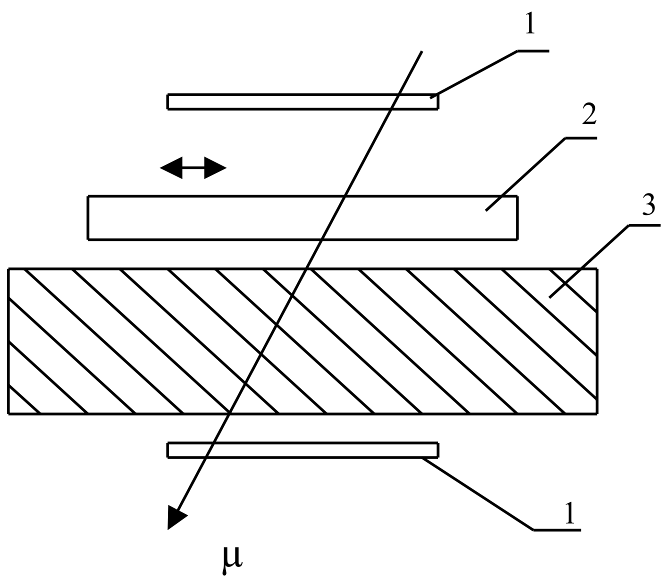


**Figure 5:** Schematic of the cosmic test stand at Dubna.

The gas mixer prepared the basic CSC gas mixture Ar+CO2+CF4 (40/50/10) with a flow of 5–30 L/h. The water-cooling system provided a water flux of 2 L/min to cool the on-chamber electronics. During testing, the CSC high voltage was varied over a range of 2.6–3.3 kV.

CSC track registration efficiency was studied with the hodoscopes' external trigger. The CSC anode track registration efficiency and noise from a single CSC layer as a function of high voltage are shown in Fig. 6. The efficiency was calculated as $\varepsilon = N_{track} / N_{trigg}$, where $N_{track}$ is the number of anode tracks reconstructed by at least 4 of the 6 CSC layers, and $N_{trigg}$ is the trigger count. One can see that the operation region lies in the range of 2.9–3.2 kV.

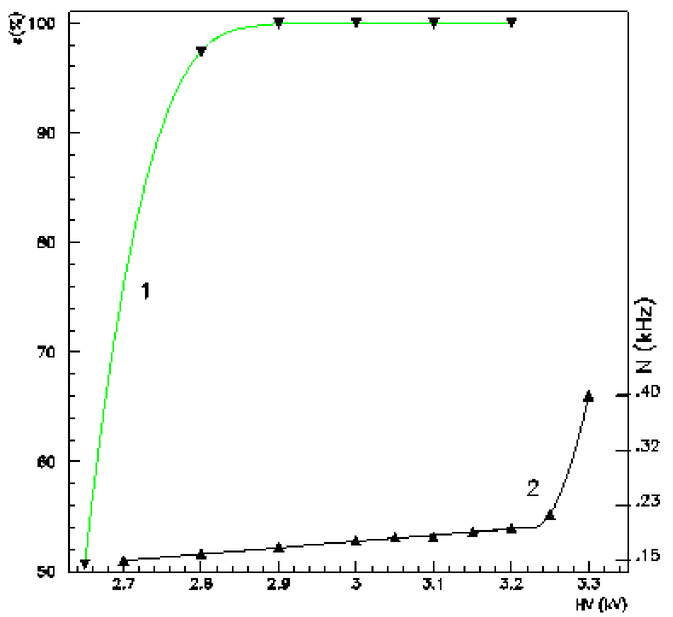


**Figure 6:** CSC anode track registration efficiency **ε** (%) (1) and layer noise N (2) vs. high voltage.

## 5. Tests after installation on the endcap disks

A number of tests were carried out after the ME1/1 CSCs took their places on the CMS detector. The layout of the ME1/1 CSCs and channel readout directions are presented in Fig. 7. Two adjacent chambers from both the West (positive) and East (negative) endcaps are shown. For all the ME1/1 CSCs the layer numbers increase from 1 to 6 going away from the interaction point (IP). The anode group numbers increase with increasing radius R. The strip numbers in the wide part (1-64) increase with increasing φ while in the narrow part the readout direction is opposite (1-16).

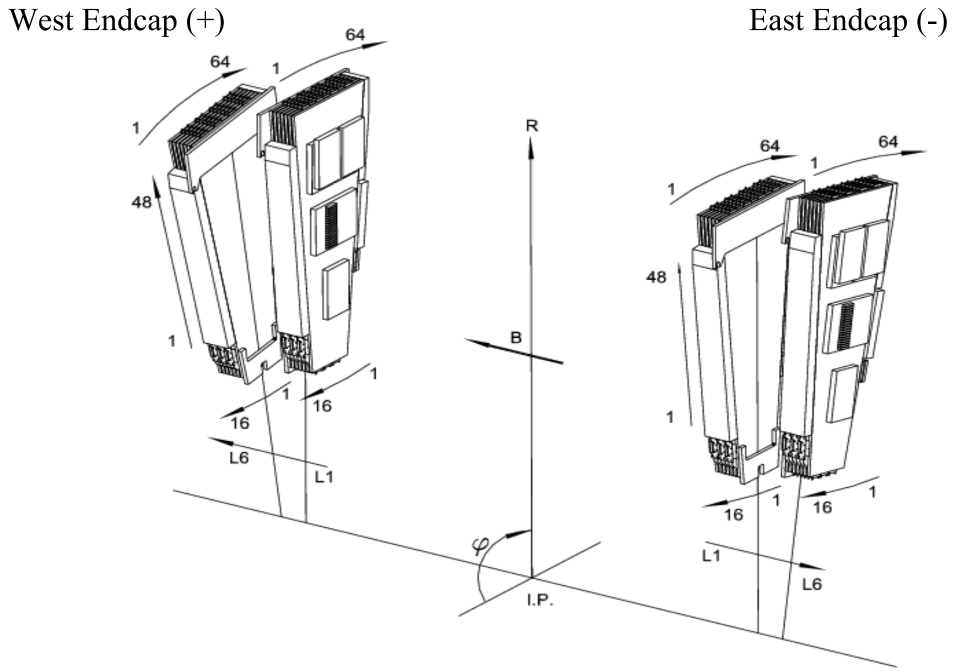


**Figure 7:** ME1/1 readout

The chambers were operated in the self-trigger regime. For cosmic-ray tests the ALCT 4/6 trigger option was taken, in which at least 4 out of 6 layers must provide coincident anode signals within a time window of 25 ns (the LHC bunch-crossing time).

The ALCT 4/6 muon trigger counting rate of ME1/1 CSCs for both endcaps was measured (Fig. 8). The radial lines indicate the centres of the 36 CSCs and show the ALCT counting rate (Hz). The maximum rate corresponds to CSC#4 installed at an angle of φ=30°. At this angle the anode wires are oriented practically vertically. One can see that in CSCs situated in the top part of the disks the counting rate is higher than for those in the bottom part. For instance, the CSC#4 rate is higher than that of CSC#22 having the same wire orientation. This asymmetry occurs because the cosmic muons reaching the bottom chamber pass more HE material than those that reach a top chamber (see Fig. 1).

The on-line display of an event is shown in Fig. 9. The cosmic muon registers in all 6 layers of the CSC. The top picture represents signal amplitudes in the strips while the bottom pictures shows the response of the anode groups. The short track that originates from layer 6 and stops in layer 3 belongs to a δ-electron.

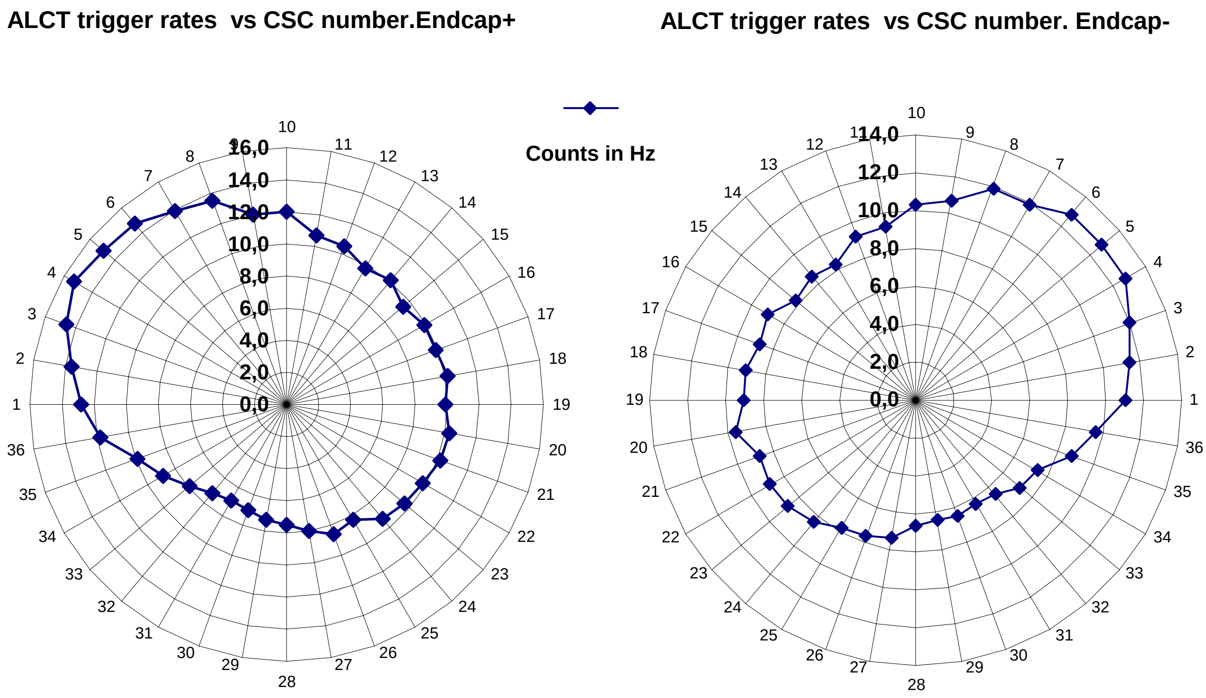


**Figure 8:** Counting rates (Hz) for CSCs (1-36) on disks, left: +Endcap, right: –Endcap.

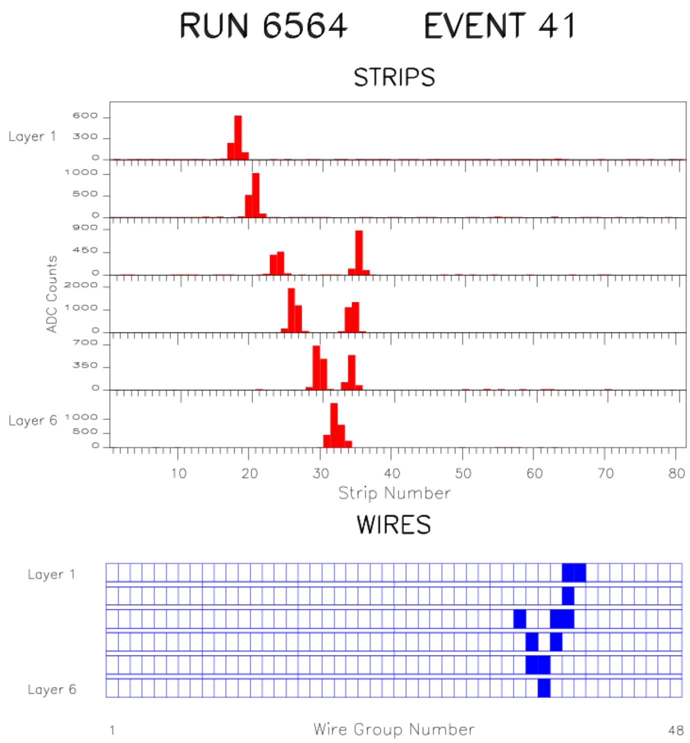


**Figure 9:** A cosmic muon registered in an ME1/1 CSC: strips (top) and anodes (bottom).

The evolution of a cluster charge in time is shown in Fig. 10 (left). The amplitudes in three neighbouring strips are plotted in 50 ns time samples. The Fig. 10 right picture shows the total cluster charge vs. high voltage for six CSC layers. One can see a good linearity of the functions and small dispersion in the charge values.

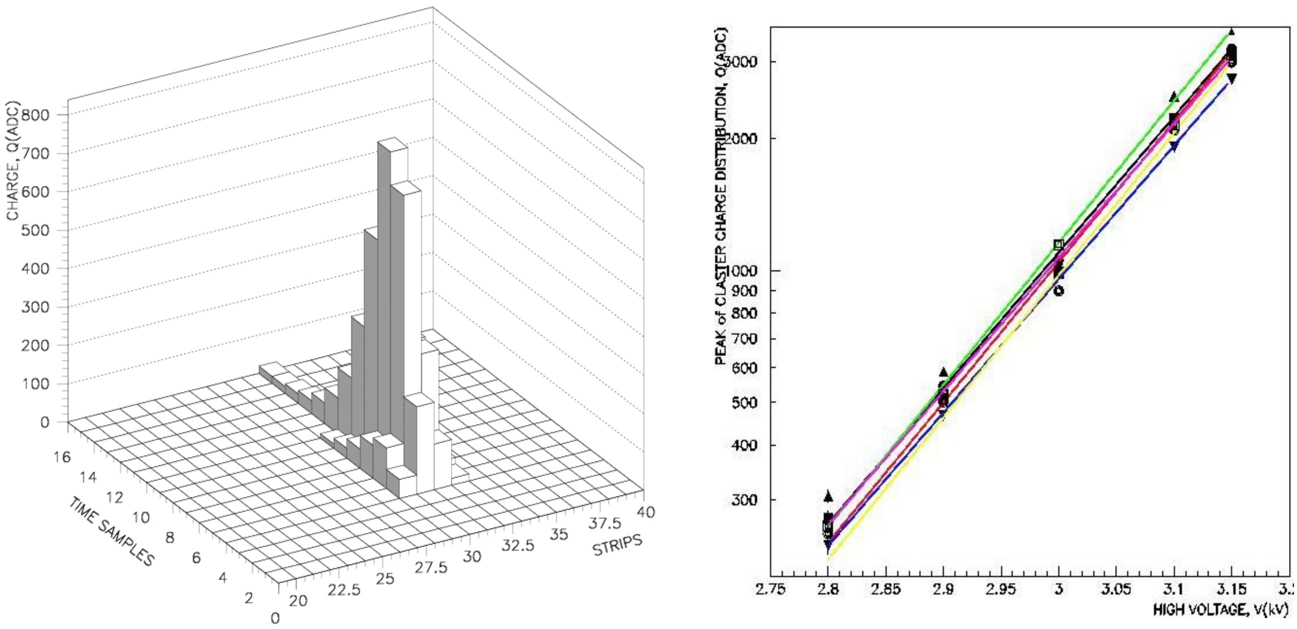


**Figure 10:** Time samples of the strip cluster charge (left); cluster charge in 6 CSC layers as a function of high voltage (right).

CSC track reconstruction efficiency as a function of high voltage was studied with the ALCT 4/6 trigger option (Fig. 11). Muon tracks were reconstructed from cathode strip data. The efficiency was calculated as $\boldsymbol{\varepsilon = N_{track} / N_{ALCT}}$, where $N_{track}$ is the number of cathode tracks reconstructed by at least 4 of the 6 CSC layers and $N_{ALCT}$ is the ALCT 4/6 count. High voltage should be fixed at 3.0 kV for all ME1/1 CSCs.

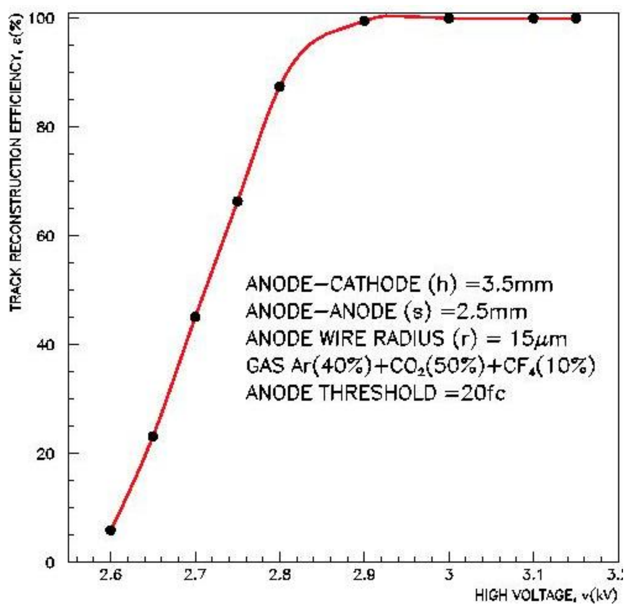


**Figure 11:** CSC track reconstruction efficiency as a function of high voltage.

## 6. Conclusion

The 76 ME1/1 cathode strip chambers (CSC) for the CMS experiment were produced at JINR. The main CSC mechanical parameters are listed. The chambers were installed in the CMS detector and commissioned. The ME1/1 electronics readout scheme is shown. The results of tests with cosmic-ray muons are presented. The layer efficiency, cathode cluster charge, and track reconstruction efficiency as a function of high voltage were studied. The chamber operating voltage for a gas mixture of Ar+CO2+CF4 (40/50/10) was determined to be 3.0 kV.

## References


1. CMS Technical Proposal. CERN/LHCC 94-38, LHCC/P1, CERN, 1994.
2. CMS Muon Technical Design Report. CERN/LHC 97-32, CMS TDR 3, CERN, 1997.
3. C. Albajar et al., NIM A364 (1995), 473–487.
4. Yu.V. Erchov et al., JINR Communic., E13-99-296, JINR, 1999.
5. Yu.V. Erchov et al., JINR Communic., E13-2000-26, JINR, 2000; http://www.jinr.ru/publish/Preprints/2000/e13-2000-26.pdf
6. I.A. Golutvin et al., Part. and Nucl. Lett. 2001, No. 4 [107], 45–53.
7. I.A. Golutvin et al., Part. and Nucl. Lett. 2001, No. 4 [107], 54–61.
8. S.A. Movchan, P.V.Moissenz, Part. and Nucl. Lett. 2001, No. 4 [107], 82–92.
9. Yu. Erchov et al., Proc. of the 7th Int. Conf. on Advanced Technology and Part. Phys. (ICATPP-7), ISBN 981-238-180-5, Singapore, 2002, 347–351.
10. K.A. Zoubov et al. JINR Communic., P10-99-118, JINR, 1999.
11. S.A. Movchan, K.P. Moissenz, P.V. Moissenz, JINR Communic., P10-2000-188, JINR, 2000.
12. I.A. Golutvin et al., Computer Phys. Communic., 126 (2000), 72–76.
13. I. Golutvin et al., Proc. of the 7th Int. Conf. on Advanced technology and Part. Phys. (ICATPP-7), ISBN 981-238-180-5, Singapore, 2002, 282–288.
14. M. Huhtinen, CMS-NOTE-2000/068, CERN, 2000.
15. A. Sannikov, A. Uzunian, CMS-NOTE-2001/018, CERN, 2001.
16. Yu.V. Erchov et al., Part. and Nucl. Lett. 2006, No.3 [132], 73–80.
17. R. Breedon et al., NIM A471 (2001), 340–347.
18. T.Y. Ling, Proc. of the $4^{th}$ Workshop on Electronics for LHC Experiments, Rome, Italy, 1998, 262–266.
19. T. Ferguson et al., Proc. of the 7th Workshop on Electronics for LHC Experiments, Stockholm, Sweden, 2001, 190-194; NIM A539 (2005), 386–406.